Fluid Dynamics inside a Mini-scale Microbial Energy Harvesting System

Way Lee Cheng[1], Kumaran Kannaiyan[1], Reza Sadr[1]*, and Arum Han[2]

Abstract—Microbial electrochemical cells are an interesting energy harvesting system that utilizes various carbon sources such as wastewater. Fluid inside the system is replenished at regular frequencies to supply nutrients to the catalytic microbes for continuous energy production. However, the replenishment process can be a challenge in micro-scale devices as the flow field inside is often laminar. Whereas, the high flow rate is not desired as the resulting high fluid shear can disrupt the catalytic microbes. To this end, the computational fluid dynamics simulations are performed to study the effect of design configurations on the replenishment efficiency. The results show that the success rate of replenishment is only about 55 % to 60 % when the inlet and outlet ports are located close to each other. The maximum efficiency obtained with the optimal design is only 70 %, which is typically not accounted for most of the experiments. Hence, there is a possibility of significant error when calculating the nutrient utilization rates, which in turn can affect the system efficiency. Furthermore, other design factors that affect the replenishment such as the distance between inlet and outlet ports and the orientation of the inlet and outlet ports are investigated.

Index Terms— Computational Fluid Dynamics, Design Optimization, Fuel Cell, Flow dynamics, Microbial Electrochemical Cells.

1 Introduction

Depletion of fossil fuel and the constant increase in the use of fossil fuel intensifies the global warming, which led several efforts for the development of clean alternative energy source such as hydrogen fuel. Recently, a few studies pointed out that a substantial amount of clean energy is bounded in organic wastes and that could be utilized to meet the growing energy demand [1], [2], [3]. Microbial electrochemical cell systems are emerging technologies that can directly convert the organic wastes into clean energy. It utilizes microorganisms as catalysts to convert the unutilized energy to produce renewable hydrogen gas through the electrolytic process [4], [5], [6], [7]. A typical design for a microbial electrolysis cell (MEC) consists of a two-compartment chamber, anode and cathode, separated by a proton exchange membrane [8]. Alternative designs such as a single-chamber configuration has also been proposed and investigated [9], [10]. MEC's are increasingly considered as a next generation carbon-neutral power source [11]. However, the widespread implementation of MECs is still limited by the economic nonviability because of their low power density. Therefore, the technology has been implemented at micro- and mini-scale systems in laboratories or at small pilot-scale commercial systems [12], [13].

The efficiency of MECs is constrained by various parameters [14], some of which are related to the system itself but many are related to their operation conditions. Significant improvements are required in materials, designs, as well as operating parameters to make them economically feasible. Large number of small-scale MEC systems are typically used in laboratory settings to achieve higher throughput. The volume of each system is typically of the order of few cubic milliliters and the substrate in that small volume has to be replenished periodically to feed the microorganisms (catalyst). The replenishment process has to be as efficient as possible to achieve higher overall system performance and at the same without washing away the microbes that reside in the anode. The performance of the MEC systems is assessed based on the substrate utilization, which depends on the volumes of substrate consumed and the hydrogen gas produced. In most cases, it is simply calculated as the replenishment volume because of the size of the system and very low flow rate of the substrate. This need not be the case all the time due to the limitation in mass transport in laminar flow regime inside the system. Consequently, this assumption can lead to a significant overestimation of nutrient utilization and in turn the MEC overall performance. This emphasizes the need for an accurate estimate of the substrate replenishment. This serves as the key motivation for the present study, where the substrate flow dynamics for different design configurations are investigated using computation fluid dynamics tool. Although a few studies made such an effort, they are system dependent and there has not been a comprehensive study on the design optimization of the MEC system reported in the literature.

Bazylak et al. concluded that rectangular cross-section MEC's with high width-to-height ratio are the optimal design with highest performance [15]. Another study showed that the performance of a micro-fuel cell can be improved for cases of high duct width-to-height ratio and higher Péclet number internal flows [16]. In a different work, a model was developed and used to simulate the bridge-shaped microfluidic fuel cell [17], where the authors concluded that further research is needed, to optimize the performance of such a system. Multiphysics and multi-chemistry methods have been proposed for a variety of micro-scale devices such as a microcombustor/reformer for hydrogen production [17] and MFC [18], [19]. However, studies of the hydrodynamics and mass transfer mechanisms of fluid flow within the anode chamber of the microbial electrochemical cell are very limited and inconclusive. The replenishment process is a transient process,

* *Reza Sadr – corresponding author: reza.sadr@qatar.tamu.edu*

[1]*Texas A&M University at Qatar, Doha, Qatar.*
[2]*Texas A&M Univeristy, College station, Texas, USA.*

which implies that the overall performance depends on the duration of the replenishment process. All the above factors serve as the motivation for the present study, which is intended to provide insights and understand the factors that affect the fluid flow as well as mass transfer within the anode chamber of a typical microbial electrochemical cell system using computational fluid dynamics tool. The influence of design parameters such as system shape, inlet and outlet port orientations on the system level performance, optimal design for such systems are investigated.

2 COMPUTATIONAL DETAILS AND METHODOLOGY

As a good starting point, a cylindrical configuration is assumed as the basic shape for the anode and cathode chambers. The anode chamber has one inlet for supplying the substrate for the microbes and one outlet for discharging the substrate. The cathode chamber is filled with stagnant fluid and has only one outlet to collect the hydrogen gas at the top. Both chambers have a headspace volume of 7 mL for collecting the gaseous species (carbon dioxide and hydrogen) produced. The dimensions of the basic cylindrical design are chosen in such a way that the volume of each of the anode and cathode chambers will be 50 mL, in lieu of the existing experimental facility at Texas A&M University. This will help to have a comparison of the flow parameters between the experimental and numerical sections. Typical geometry for the anode chamber of the MEC illustrated in Fig. 1 is analyzed for the optimization purpose. The chamber is assumed to be initially filled with the old substrate fluid. Unless otherwise stated, the anode chamber is assumed to confirm with the specifications shown in Table. 1.

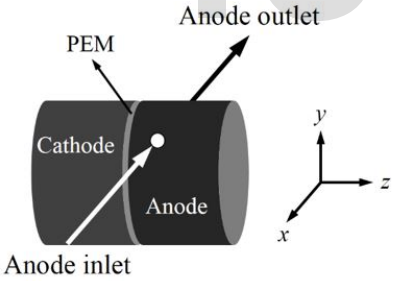

Fig. 1. An illustration of a cylindrical shape micro electrolysis cell design.

Table 1. Geometric specifications of the anode chamber

Chamber diameter	50 mm
Chamber width	25 mm
Chamber volume	50 mL
Filling time[A]	2 hr, 4 hr, 6 hr
Substrate mass flow rate	5.976 mg/s
Inlet and outlet port diameter	3 mm

[A] Time required in filling 43 g of new substrate.

Chemical reactions inside the chambers are ignored due to the slow production rate of gases. Since the focus of the present numerical simulation is primarily on the flow fields within the anode chamber for design optimization, the cathode chamber is excluded in all the simulations presented in this work. Neglecting the cathode chamber reduces the computational time by at least 50%. The governing equations for incompressible laminar flow, transient, constant properties and isothermal, is given by the simplified Navier-Stokes equations,

$$\nabla \cdot \boldsymbol{u} = 0 \tag{1}$$

$$\frac{\partial \boldsymbol{u}}{\partial t} + \boldsymbol{u} \cdot \nabla \boldsymbol{u} = -\nabla p + \mu \nabla^2 \boldsymbol{u} \tag{2}$$

where, p is the pressure, $\boldsymbol{u}$ is the velocity vector and μ is the dynamic viscosity. Species transport is given by,

$$\frac{\partial \rho C_j}{\partial t} + \nabla \cdot \left(\rho \boldsymbol{u} C_j\right) = -\nabla \cdot \boldsymbol{J}_j \tag{3}$$

where C_j is the local mass fraction of species j in the mixture, ρ is the fluid density and $\boldsymbol{J}_j$ is the diffusive flux of species j into the mixture, which is given by the Fick's Law, invoking the dilute solution assumption, is given by,

$$\boldsymbol{J}_j = -\rho D_j \nabla C_j \tag{4}$$

where D_i is the diffusion coefficient of species j into the mixture. In general, an analytical solution is not available for (1) to (4). The governing equations are numerically solved using ANSYS-FLUENT. Initially three geometric configurations are considered to study the effect of inlet location and angle of incoming fluid in the radial direction (as summarized in Fig. 2) on the prediction of new substrate mass flow pattern.

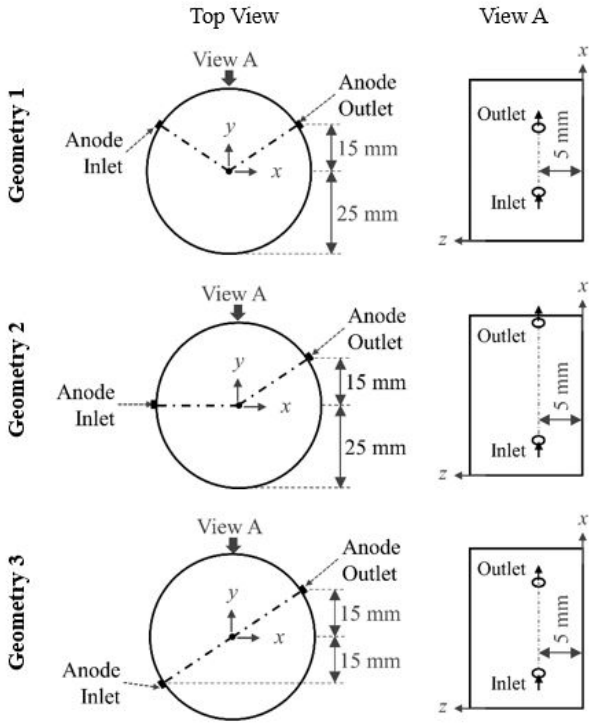

Fig. 2. Schematic of different inlet/outlet port configuration investigated.

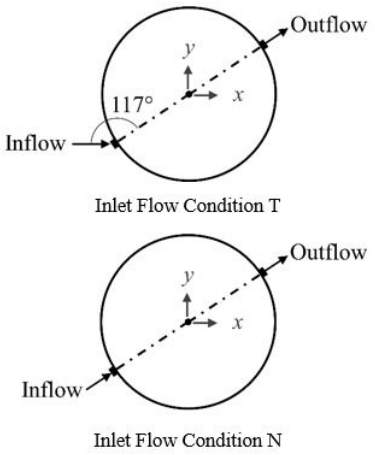

Fig. 3. Schematic of different inlet flow condition.

Two inlet flow conditions are considered in this study, as shown in Fig. 3, Inlet Flow Condition T represents the fluid velocity is fixed in +x-direction and, Inlet Flow Condition N indicates that the inlet flow velocity is normal to the anode chamber wall surface.

Table 2. Design configurations of the anode chamber.

Case	Geometry	Inlet Flow Condition
I	1	T
II	1	N
III	2	T
IV	3	T

Table 2 summaries the cases considered in this section. The filling time (T_f) for 43 g of fresh substrate is assumed to be two hours based on the experimental details.

2.1 Grid Independence study

For the grid independent study, several computational grids with a cell count between 1×10^5 and 1.6×10^6 cells (an order of magnitude increase) are considered for the cases I and IV. The mass balance between the inlet and outlet ports, and residual value of new-substrate mass are taken as the convergence metrics. The system level mass balance (i.e., difference in mass flow rate between inlet and outlet) is within 0.1% for all the cases studied. Also, the residual value, the difference in mean value of the variable between successive iterations, is at least two orders of magnitude lower than the inlet mass flow rate. Fig. 4 shows the effect of grid size on the prediction of new substrate mass (m_{NS}) inside the anode chamber, which is presented as a percentage of the total mass of the anode chamber. It is evident that the mesh with a cell count of 4×10^5 cells is able to predict the trend and values of the new substrate mass inside anode chamber volume as that of higher cell count. Therefore, for all other studies the mesh with a cell count of 4×10^5 cells is used.

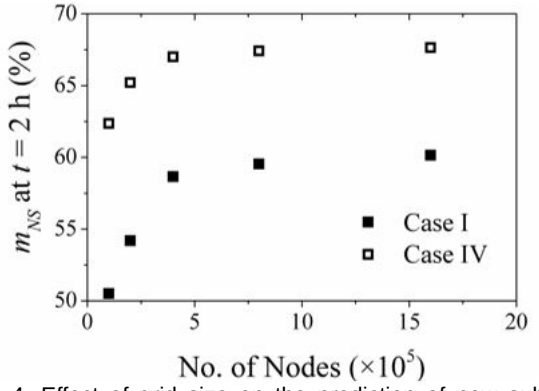

Fig. 4. Effect of grid size on the prediction of new substrate mass percentage.

2.2 Effect of time step

The next important parameter is the time step size for the transient simulations. In this study, the time step size (Δt) has been varied from 4 to 0.5 seconds and its influence on the prediction of new substrate mass is investigated using case IV. The results indicate that the change in time step size has not influenced the prediction of new substrate mass inside anode chamber volume as shown in Fig. 5. The time (x-axis) is normalized using the time to fill the chamber volume of 43 mL (T_f). In all the cases, the residual value of the new substrate mass is three orders of magnitude less. Therefore, for all the studies a time step size of 4 seconds is chosen.

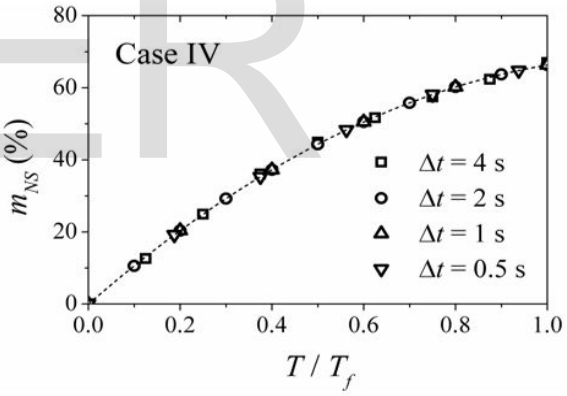

Fig. 1. Effect of time step size on the prediction of new substrate mass (m_{NS}).

3 Results and Discussions

Numerical simulations are carried out for each of the four simulation conditions in Table 2 using a mass flow rate of 5.97 mg/s, which represent the two-hour case. Fig. 6 shows the comparison of new-substrate mass predicted inside the anode volume over time for various cases. It is clear that the difference in the new-substrate mass prediction is less between cases I and II, when compared to the difference between case I and IV. However, the new-substrate mass prediction in case I is much lower than those predicted for cases III and IV. The differences in new-substrate mass prediction between the cases highlight the effect of inlet location and flow orientation. Furthermore, the path-lines (defined as flow path traced by the fluid particles) predicted for different geometries are compared in Fig. 7. The

flow path-lines are colored by the velocity in x-direction with magnitude varying from 0 to 0.005 mm/s.

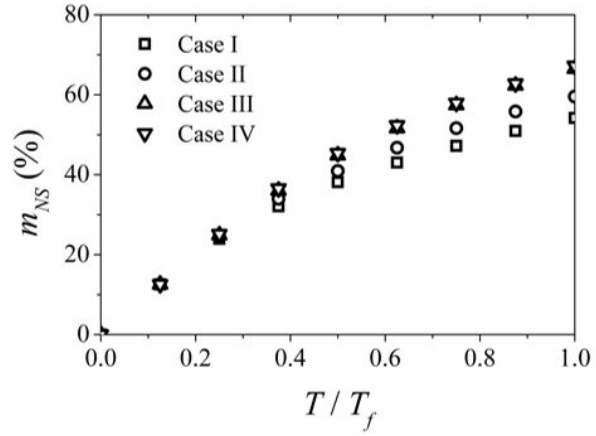

Fig. 6. Comparison of fresh substrate mass (m_{NS}) as a percentage of total mass inside anode chamber predicted over time for different geometric configurations (inlet mass flow rate is 5.973 mg/s and T_f equals to two hours).

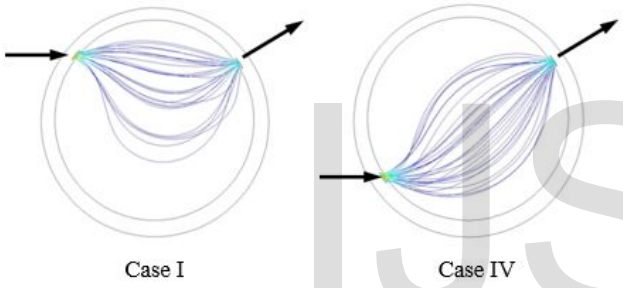

Fig. 7. Comparison of path-lines predicted for different geometry configurations, cases I and IV.

In both case I and case II, most of the new substrate fluid is flowing across the chamber and leaves through the outlet port. In case IV, where the inlet and outlet ports are located diagonally opposite to each other, provides the longest path for the new substrate fluid flowing across the chamber and improves the new substrate fluid retention rate. The simulations performed with flow conditions pertaining to the two-hour case show that the geometric configuration with the inlet and outlet ports positioned diagonally opposite to each other shows a better retention (performance) of fresh substrate mass when compared to the other two geometric configurations. Although case IV shows better retention of new-substrate mass, the amount of new-substrate mass retained inside the anode chamber after two hours is only 70% of the mass of total incoming substrate fluid, while this has been conventionally regarded as 100%. This highlights that the design could be further optimized to retain additional fresh substrate mass inside the anode chamber.

The effect of inlet mass flow rate on the prediction of new-substrate mass inside the anode volume is studied by considering two extreme cases of inlet flow configurations (case I and IV). The time considered to fill the anode chamber are 2, 4, and 6 hours and the respective mass flow rates are 5.976, 2.986, and 1.991 mg/s. Fig. 8 shows the effect of inlet mass flow rate on the predicted new-substrate mass percentages inside the anode chamber volume over time. The trends are similar across the mass flow rates for both cases, as shown in Fig. 8. It is evident from Fig. 8 that the time considered (and mass flow rate) to replenish the anode chamber is insensitive until T/T_f, reaches 0.6.

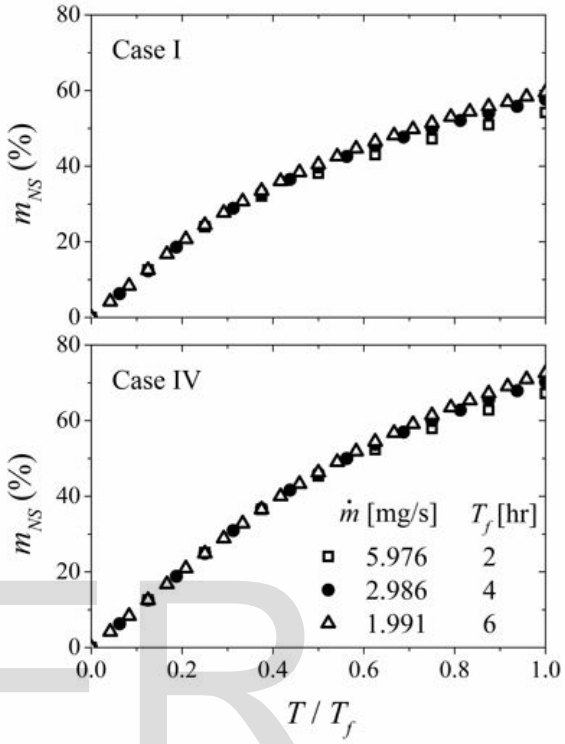

Fig. 8. Comparison of the predicted fresh substrate mass (m_{NS}) inside the anode chamber volume at different mass flow rates over time for case I (top) and case IV (bottom).

In case IV, the new-substrate mass can be retained inside the anode chamber up to a maximum of 70% of the anode chamber volume, whereas in case I, it can only reach up to a maximum of 60%. For a given geometric configuration, the flow patterns (i.e. flow path-lines) are similar between the mass flow rate cases. Overall, the case IV showed a better performance than case I, although the trends are similar. The amount of new-substrate mass retained inside the anode chamber volume increases with higher mass flow rate. However, increasing the mass flow rate is not desired as it may wash away the microbes inside the anode due to high wall shear exerted at higher fluid velocity. Therefore, optimizing the geometry would be a better way to increase the retention of fresh substrate fluid mass. In view of this, it may be worth performing numerical simulations by changing the location of the inlet port in such a way that the inlet and outlet ports are not located in the same xy-plane.

Geometry 3, which showed the best performance in retaining the incoming fresh substrate fluid, is considered to investigate the influence of inlet/outlet ports location on the flow field. Fig. 9 shows the chamber configurations considered in this part of the study, *i.e.*, geometry 3 as shown in Fig. 2; geometry 4 is the modified geometry 3, where the inlet/outlet

ports are located on different planes; and geometry C is a cubic chamber that is also used in some experimental work. The volume of all the chambers is 50 mL and the fluid filling time is two hours for all cases. Table 4 summarizes the chamber geometry and inlet flow conditions considered here.

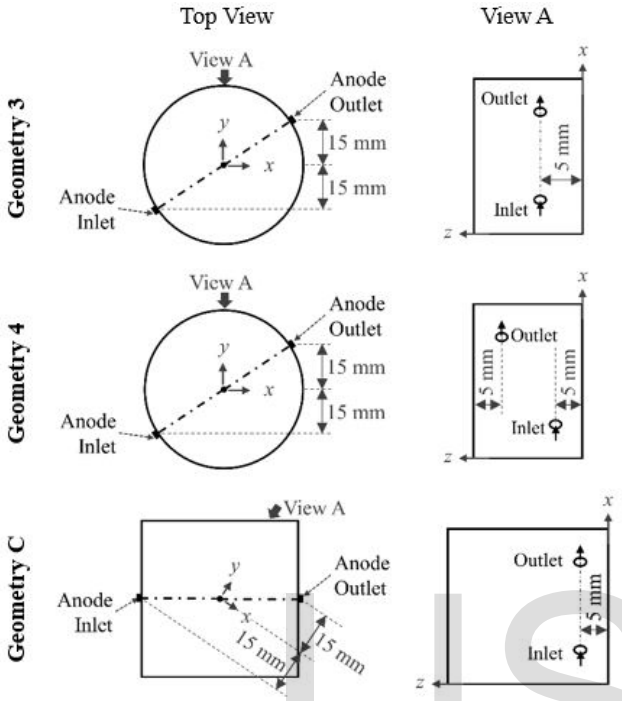

Fig. 9. Different anode chamber configurations considered for design optimization.

Table 3. Simulation specifications of optimizing the chamber design for fresh substrate retention.

Case	Geometry	Inlet Flow Condition
IV	3	T
V	4	T
VI	4	N
C	C	T

Fig. 10 shows the predicted fresh substrate mass within the anode chamber over time. The cylindrical chambers (cases IV, V and VI) have better replenishment performance when compared to the cubic chamber. After two hours of filling, the cubic chamber has only 48% of new substrate mass, while both the cylindrical chambers showed over 65% of replenishment. Meanwhile, by not aligning the inlet and outlet ports in geometry 4, the replenishment rate is increased from 67% in case IV to 69% in case V and 72% in case VI. It is interesting to note that in Fig. 10 the fluid retention for geometry 4 with different inlet fluid velocity vector shows the opposite trend to that of geometry 1 (shown in Fig. 6).

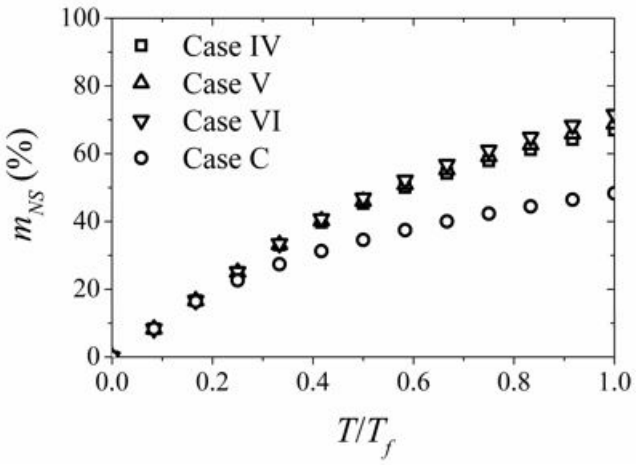

Fig. 10. New substrate mass predicted (T_f = 2 hours) for different design configurations.

For geometry 4, higher replenishment is observed by considering the inlet flow direction normal to the chamber wall. In contrast, higher fluid retention is observed in geometry 1 when the inlet flow is aligned in the +x-direction. Fig. 11 shows the contours of mass concentration of new substrate overlaid with fluid flow pattern inside the anode chamber after two hours of substrate filling.

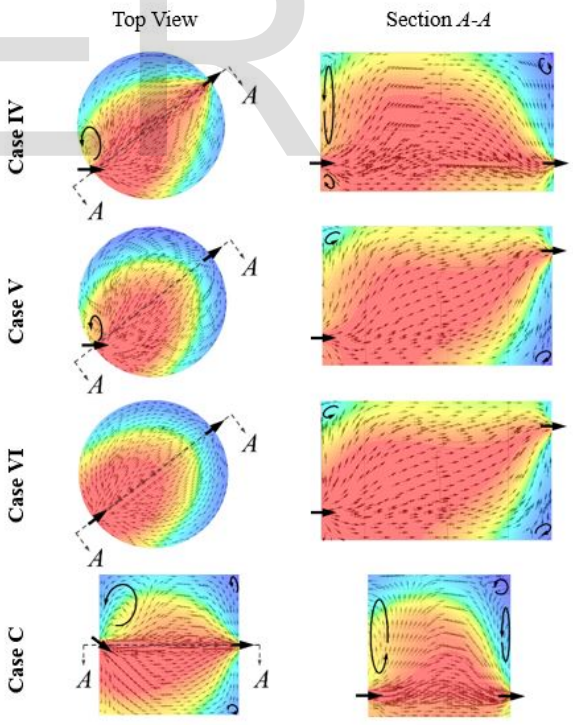

Fig. 11. Contours of new substrate mass fraction within the anode chamber after two hours of filling overlaid with velocity distribution. Red and blue colors represent the concentration of new and old substrate fluid mass, respectively.

The top-view is the cross-section at z = 5 mm (across the inlet port). Section A-A is the cross-section connecting the inlet

and outlet ports for each of the cases. The elliptic arrow shows the location and direction of eddy recirculation within the chamber. The mass concentration trends are consistent with the results shown in Fig. 10. From the figure, it is observed that by perfectly aligning the inlet and outlet ports, the incoming fluid has a tendency of simply passing through the chamber instead of replenishing the substrate fluid inside the chamber. This can be seen in Fig. 11 as a large portion in the top-portion of section *A-A* for both geometry 3 and geometry C has lower concentration of the new-substrate, comparing to those for Geometry 4. In addition, the retention of the new substrate mass within the chamber is much lower for the cubic chamber, which has a shorter distance between the inlet and outlet ports than that of the cylindrical chamber. It is important to that recirculation zones, which correspond to low concentration of new substrate mass, exist in all fours cases. They are mostly developed in the corner regions of the chambers as well as in the trailing region relative to the inlet fluid flow. The only mechanism that replaces these circulating fluids is diffusion, which is several orders of magnitudes slower than mixing and convection. The results indicate that the stronger the recirculation zone, the lower the overall fluid replenishment.

Comparing the profiles for cases IV (geometry 3), V and VI (both geometry 4), case IV has a strong recirculation zone close to the inlet port that extends throughout the height of the chamber. Case V has a relatively weaker recirculation zone next to the inlet port. However, it does not extend in *z*-direction as seen in case IV, except for a very narrow region close to the chamber wall. In comparison, for case VI, when the incoming fluid is directed through the inlet port normal to the chamber wall, the incoming flow is dispersed in a symmetric manner. This results in no obvious recirculation regions being generated neighboring to the inlet port of the chamber. The only recirculation zones for case VI are the ones in the corners (see section *A-A*), which justifies the higher replenishment for case VI as most of the fluid is convected through the chamber, instead of pure diffusion. Finally, non-alignment of the inlet and outlet ports leads to a longer fluid path and in turn longer duration of mass exchange between the new and old substrate fluids.

4 Conclusions

Numerical simulations were performed to investigate the influence of design parameters on the new substrate mass flow pattern inside the micro electrolysis cell. The results from this work clearly demonstrated that the location of inlet and outlet ports and the orientation of incoming fluid to the inlet surface are crucial to improve the fresh substrate mass retention inside the MEC chambers. Cylindrical shape chambers showed better retention efficiency when compared to their cubical counterparts. In cylindrical chambers, placing the inlet and outlet ports on different planes is seen to enhance the retention efficiency owing to longer residence time of the new substrate mass. Interestingly, it is also shown that the retention of new substrate fluid is only marginally affected when the time to fill the chamber is increased from two hours to six hours. However, higher substrate velocity may not be desired as it might wash away the microorganisms because of high wall shear. Furthermore, it is also important to reduce the possibility/proportion of the recirculation zones inside the chamber, where the mass exchange is dominated by slow diffusion process. By aligning the direction of incoming fluid normal to the chamber wall, it is possible to completely eliminate a strong recirculation zone in the vicinity of the inlet port to further improve the replenishment. All these results clearly highlight the scope for increasing the substrate replenishment and in turn the overall performance by further optimizing the design. Therefore, additional investigations are warranted to study the influence of shape and size of the inlet and outlet ports.

5 Funding

This work was supported by the Qatar National Research Fund (a member of the Qatar Foundation) under Grant NPRP 5-671-2-278.

6 Acknowledgment

The High Performance Computing resources and services used in this work were provided by the IT research computing group at Texas A&M University at Qatar.

7 References

[1] B.E. Logan, and K. Rabaey, "Conversion of Wastes into Bioelectricity and Chemicals by Using Microbial Electrochemical Technologies". Science, vol. 337, no. 6095, pp. 686, 2012.

[2] B.E. Logan, "Peer Reviewed: Extracting Hydrogen and Electricity from Renewable Resources", Environ. Sci. Technol. Vol. 38, no. 9, pp. 160A-167A, 2004.

[3] P.L. McCarty, J. Bae, and J. Kim, "Domestic Wastewater Treatment as a Net Energy Producer–Can This be Achieved?", Environ. Sci. Technol., vol. 45, no. 17, pp. 7100-7106, 2011.

[4] H. Liu, S. Grot, and B.E. Logan, "Electrochemically Assisted Microbial Production of Hydrogen from Acetate", Environ. Sci. Technol., vol. 39, no. 11, pp. 4317-4320, 2005.

[5] R.A. Rozendal, H.V.M. Hamelers, G.J.W Euverink, S.J. Metz, C.J.N. Buisman, "Principle and perspectives of hydrogen production through biocatalyzed electrolysis", Int. J. Hydrogen Energy, vol. 31, no. 12, pp. 1632-1640, 2006.

[6] B.E. Logan, and J.M. Regan, "Microbial Fuel Cells-Challenges and Applications", Environ. Sci. Technol., vol. 40, no. 17, pp. 5172-5180, 2006.

[7] B.E. Logan, D. Call, S. Cheng, H.M.V. Hamelers, T.H.J.A. Sleutels, A.W. Jeremiasse, R.A. Rozendal, "Microbial Electrolysis Cells for High Yield Hydrogen Gas Production from Organic Matter", Environ. Sci. Technol., vol. 42, no. 23, pp. 8630-8640, 2008.

[8] H. Liu, H. Hu, J. Chignell, Y. Fan, "Microbial electrolysis: novel technology for hydrogen production from biomass", Biofuels, vol. 1, no. 1, pp. 129-142, 2010.

[9] D. Call, and B.E. Logan, "Hydrogen Production in a Single Chamber Microbial Electrolysis Cell Lacking a Membrane", Environ. Sci. Technol., vol. 42, no. 9, pp. 3401-3406, 2008.

[10] H. Hu, Y. Fan, and H. Liu, "Hydrogen production using single-chamber membrane-free microbial electrolysis cells", Water

Research, vol. 42, no. 15, pp. 4172-4178, 2008.

[11] B. He, J. Wang, S. Huang, Y. Wang, "Low-carbon product design for product life cycle". J. Engg. Design, vol. 26, no. 10-12, pp. 321-339, 2015.

[12] L.T. Angenent, K. Karim, M.H. Al-Dahhan, B.A. Wrenn, R. Domiguez-Espinosa, "Production of bioenergy and biochemicals from industrial and agricultural wastewater", Trends in Biotechnology, vol. 22, no. 9, pp. 477-485, 2004.

[13] B.H. Kim, I.S. Chang, and G.M. Gadd, "Challenges in microbial fuel cell development and operation", App. Microbiology and Biotechnology, vol. 76, no. 3, pp. 485, 2007.

[14] K. Rabaey, and W. Verstraete, "Microbial fuel cells: novel biotechnology for energy generation", Trends in Biotechnology, vol. 23, no. 6, pp. 291-298, 2005.

[15] A. Bazylak, D. Sinton, and N. Djilali, "Improved fuel utilization in microfluidic fuel cells: A computational study", J. Power Sources, vol. 143, no. 1–2, pp. 57-66, 2005.

[16] M.H. Chang, F. Chen, and N.-S. Fang, "Analysis of membraneless fuel cell using laminar flow in a Y-shaped microchannel". J. Power Sources, vol. 159, no. 2, pp. 810-816, 2006.

[17] S.R. Deshmukh, and D.G. Vlachos, "CFD Simulations of Coupled, Countercurrent Combustor/Reformer Microdevices for Hydrogen Production", Industrial and Engineering Chemistry Research, vl. 44, no. 14, pp. 4982-4992, 2005.

[18] Y. Zeng, Y.F. Choo, B.H. Kim, P. Wu, "Modelling and simulation of two-chamber microbial fuel cell", J. Power Sources, vol. 195, no. 1, pp. 79-89, 2010.

[19] C. Picioreanu, I.M. Head, K.P. Katuri, M.C.M Van Loosdrecht, K. Scott, "A computational model for biofilm-based microbial fuel cells", Water Research, vol. 41, no. 13, pp. 2921-2940, 2007.